Journal of the European Ceramic Society 20 (2000) 185–193

Sintering of $LaCoO_3$ based ceramics

K. Kleveland, M.-A. Einarsrud, T. Grande*

Department of Chemistry, Norwegian University of Science and Technology, 7491 Trondheim, Norway

Received 18 January 1999; received in revised form 22 April 1999; accepted 11 May 1999

Abstract

The densification, microstructure and phase evolution of near stoichiometric, Co-excess and Co-deficient perovskite $La_{1-x}M_xCoO_{3-\delta}$ (M = Ca, Sr; $x = 0$, 0.2) powders have been investigated by electron microscopy and powder X-ray diffraction. Sub-micron powders were prepared from nitrate precursors using the glycin-nitrate and the EDTA methods. The sintering temperature was observed to decrease with Ca or Sr substitution. Dense materials with grain size in the order of 3–5 μm have been obtained at 1200°C for near stoichiometric powders. Considerable grain growth was observed at higher sintering temperatures. The presence of other crystalline phases in addition to the perovskite due to Co-excess/-deficiency considerably affects the microstructure and acts as grain growth inhibitors by grain boundary pinning. The volume fraction of secondary phases is particularly large in the case of Co-deficient $LaCoO_3$ due to the formation of $La_4Co_3O_{10}$. In non-stoichiometric $La_{0.8}Ca_{0.2}CoO_3$, a liquid phase consisting mainly of CaO and CoO was observed at 1400°C causing exaggerated grain growth. Considerable pore coarsening was observed in Co-excess $La_{0.8}Ca_{0.2}CoO_3$ at 1350°C. The present investigation demonstrates the importance of controlling the stoichiometry of $LaCoO_3$ based ceramics in order to obtain dense materials with well defined microstructure.

Keywords: Grain growth; $LaCoO_3$; Microstructure-final; Perovskites; Sintering

1. Introduction

Mixed ionic and electronic conducting perovskites $La_{1-x}M_xCoO_{3-\delta}$ (M = Ca, Sr) have potential application as materials for oxygen permeable membranes, electrodes, oxidation catalysts and oxygen sensors.[1–6] In order to achieve the functional properties required for an oxygen permeable membrane, dense materials with well defined microstructure is desired. In most cases the presence of secondary phases will decline the functional properties of the membrane, and therefore single phase materials are preferred. The mechanical properties might also be critical if oxygen is produced by applying a pressure gradient over the membrane or if thin membranes are desired in order to achieve sufficient oxygen flux. The purpose of this study was to investigate the sintering behaviour of $LaCoO_3$ based ceramics. The effect of substitution and cation stoichiometry on the sintering properties has been investigated in the temperature interval 1050–1450°C.

Sintering of $LaCoO_3$ based ceramics has not been investigated thoroughly. Koc et al.[7] investigated the sintering behaviour of $La_{1-x}Ca_xCr_{1-y}Co_yO_3$, and they obtained a maximum density of 95% of theoretical density for both $LaCoO_3$ and $La_{0.7}Ca_{0.3}CoO_3$. Decreased sintering temperature by substitution of Ca was reported. Denos et al.[8] investigated the relationship between green and fired densities for $LaCoO_3$ and $La_{0.5}Sr_{0.5}CoO_3$. Higher densities were reported for $LaCoO_3$ than for the strontium substituted $LaCoO_3$.

Phase equilibrium in the La–Co–O system in the temperature interval 800–1200°C has been studied by several authors.[9–13] Stable ternary oxides observed in the system are $LaCoO_3$, La_2CoO_4 and $La_4Co_3O_{10}$. $LaCoO_3$ decomposes to CoO and $La_4Co_3O_{10}$ at low oxygen partial pressures. There are conflicting reports on the solid solution of La_2O_3 or CoO in $LaCoO_3$. Morin et al.[14] report the presence of secondary phases at more than 0.3% deviation from the A/B ratio in the ideal perovskite (ABO_3). Seppänen et al.[12] claim a stability range for $LaCoO_{3-\vartheta}$ within ±1%. Munakata et al.[15] have however reported preparation of single phase $La_{0.9}CoO_3$. Since a small tolerance in A/B ratio is

* Corresponding author.
E-mail addresses: tor.grande@chembio.ntnu.no (T. Grande).

0955-2219/00/$ - see front matter
PII: S0955-2219(99)00141-7

reported in most cases, secondary phases might be difficult to avoid in the preparation of $LaCoO_3$ based ceramics. In this paper the cation stoichiometry has been varied between Co-excess and Co-deficiency in order to investigate the effect of secondary phases on the sintering behaviour.

2. Experimental

Pure $LaCoO_3$ and Sr or Ca substituted $LaCoO_3$ powders, $La_{1-x}M_xCoO_{3-\partial}$ (M = Ca, Sr; $x = 0$, 0.2), were prepared by the glycine nitrate method (G/N) described by Chick et al.[16] and the EDTA-method described here. Samples prepared from the two methods are termed G/N-samples and EDTA-samples, respectively. In addition to the near stoichiometric powders, 5 mol% Co-excess and 10 mol% Co-deficient powders were prepared. For convenience, in the following the compositions $La_{0.8}Ca_{0.2}CoO_3$ and $La_{0.8}Sr_{0.2}CoO_3$ are termed 20%Ca and 20%Sr, respectively.

Approximately 1 M solutions of the nitrate salts were used and the concentration of the solutions was measured by an Atom Scan 16 1CP-AES Spectrometer (ICP) (Thermo Jarrell Ash Corp.). In case of the G/N-method approximately 25 ml of the glycine-nitrate solution was transferred to a quartz container and then heated on a hot plate until ignition. The EDTA-powders were prepared by mixing either 1 M nitrate solutions or weighted amounts of nitrate salts, EDTA and water to a total volume of about 400 ml. The stoichiometry of the nitrate salts was determined by thermogravimetrical analysis. pH was adjusted to 9–10 with NH_4OH solution to prevent precipitation. The solution was transferred to a beaker on a hot plate, and heated at 80°C until gel formation. The gel was dried in air at 200–240°C for 24 h, and organic residue was burnt off at 600°C for 24 h.

The powders were ball milled (Si_3N_4-balls) for 4 h in 100% ethanol. The milled powders were further calcined at 900–1000°C for 8–72 h in flowing synthetic air and further ball milled for 24 h. Powder pellets (0.7 g) were uniaxially pressed (double action) at 230 MPa for GLN-powders and 70–100 MPa for EDTA-powders. The relative green density obtained was 50–55% of theoretical density.

The chemical composition of the powders was measured by ICP and is given in Table 1. X-ray powder diffraction (XRD) of powders and crushed sintered samples was performed on a Siemens D5005 diffractometer (CuK_α radiation and a secondary monochromator) in the 2θ range 20–65° with step 0.040° and step time 9.0 s. Cell parameters and crystallographic densities were calculated using the programs Profile, WinIndex and Metric. Si (20 wt%) was added the powders as an internal standard.

Table 1
Cation stoichiometry (±2%) relative to Co of the different powders

Sample composition	La	Sr	Ca	Co
EDTA-samples				
Stoichiometric				
$LaCoO_3$	1.02			1.00
20%Sr	0.80	0.204		1.00
20%Ca	0.80		0.213	1.00
Co-deficient				
$LaCoO_3$	1.12			1.00
20%Sr	0.88	0.223		1.00
20%Ca	0.87		0.205	1.00
Co-excess				
$LaCoO_3$	0.95			1.00
G/N-samples				
Stoichiometric				
$LaCoO_3$	1.01			1.00
20%Sr	0.79	0.198		1.00
20%Ca	0.80		0.207	1.00

The surface area of the powders was measured by the BET method (ASAP 2000, Micromeritics). The surface area of the G/N-powders was in the range 1.6–2.2 m^2/g, and the corresponding calculated particle size is 0.4–0.5 μm assuming spherical particles. SEM analysis shows a particle size below 2 μm, where 20%Ca has slighty larger particles than the two other compositions. The particle size for the EDTA-powders was below 1 μm determined by SEM. Surface areas were 2.9–5.0 m^2/g, and the estimated particle size assuming spherical particles was 0.2–0.3 μm.

The uniaxially pressed pellets were sintered in air at 1050–1450°C for 2–96 h. The samples were heated at 300 K/h up to the maximum temperature and cooled down to 400°C at 1000 K/h.

Dilatometry (Netch Dilatometer 42OE) was performed on uniaxially pressed pellets (115 MPa). The green dimensions of the pellets were 1.0 cm diameter and height 0.7 cm. The dilatometry was performed in ambient air at a heating rate of 120 K/h.

Fractured, polished and etched cross-sections of sintered pellets were investigated by SEM (Zeiss DSM 940) and Energy Dispersive Spectroscopy (EDS) (Noran Instruments, Tracor Series 11). The polished surfaces were prepared by grinding with SiC-papers followed by polishing with diamond particles down to 1 μm. In order to visualize the grain boundaries, the polished samples were either etched in 6 M HCl for 1–4 min or thermally etched at 1050°C for 10 min. An estimate for the grain size was obtained by measuring the maximum 2-dimensional diameter of 20–50 grains on SEM images, and the mean values were reported as average grain size.

The density of G/N-samples was calculated from the weight and geometric volume of the sintered pellets while the density of EDTA-samples was measured by the "Archimedes" method in iso-propanol.

3. Results and discussion

3.1. Phase composition

Phases observed in addition to the perovskite phase in calcined powders and sintered ceramics are given in Table 2.

3.1.1. $LaCoO_3$

The phase compositions of near stoichiometric and non-stoichiometric $LaCoO_3$ powders were in accord with the equilibrium phase diagram of the La–Co–O system.[12] Co_3O_4 and $La(OH)_3$ were observed in, respectively, Co-excess and Co-deficient powders. Due to the high reactivity with moisture $La(OH)_3$ was probably formed from La_2O_3 during cooling or at ambient temperature. La_2O_3 in Co-deficient $LaCoO_3$ sintered at 1350°C is also clearly evident as lighter grains in Fig. 1a.

At Co-deficiency the phase composition during sintering was observed to change due to the redox-reaction:

$$1/2\ La_2O_3(s) + 3\ LaCoO_3(s) = La_4Co_3O_{10}(s) + 1/4\ O_2(g) \quad (1)$$

At 1450°C close to one third of the Co-deficient sample consists of rod-shaped grains of $La_4Co_3O_{10}$ as shown in Fig. 1b. However, equilibrium has not been reached and minor amounts of La_2O_3 are still present even after 2 h at 1450°C. 10 mol% Co-deficiency corresponds to 34 vol% $La_4Co_3O_{10}$ which is in good agreement with the observation. The coexistence of $La_4Co_3O_{10}$ and $LaCoO_3$ in air at 1450°C is in agreement with an extrapolation of the phase diagram reported by Petrov et al.[13] and Seppänen et al.[12]

In Co-excess $LaCoO_3$, Co_3O_4 was observed to decompose to CoO during sintering above 900°C in accordance with the Co–O phase diagram.[17] CoO was observed to oxidize in the powders during cooling to room temperature, but oxidation during cooling did not take place in dense $LaCoO_3$ ceramics.

3.1.2. 20%Sr

The phase composition of the calcined near stoichiometric and Co-deficient 20%Sr powders are also included in Table 2. The near stoichiometric powders contained only the perovskite phase according to the XRD analysis. At Co-deficiency minor amounts of $(La,Sr)_2CoO_4$ was observed in addition to the perovskite. The chemical composition of the K_2NiF_4 type phase was $(La_{0.6}Sr_{0.4})_2CoO_4$ according to the EDS analysis of sintered bodies. Hence, the Sr content in the $LaCoO_3$ phase is probably lower than 20 mol%. Pure La_2CoO_4 is not stable in air,[12] but the substitution of La by Sr probably results in replacement of Co(II) by Co(III), and the K_2NiF_4-type phase is therefore stabilized in air. The phase composition

Table 2
Phases observed in addition to the main perovskite phase in the calcined powders and sintered samples

Sample composition	Phases observed[a,b]				
	Calcined powder 900–1000°C	1200°C	1350°C	1400°C	1450°C
EDTA-samples					
Stoichiometric					
$LaCoO_3$	(none)	(*La_2O_3*, *La–Si–O*)	(*La_2O_3*, *La–Si–O*)	–	–
20%Sr	(none)	(*Sr–s*)	(*Sr–S*)	–	–
20%Ca	(none)	(*CoO*)	(*CoO*)	–	–
Co-deficient					
$LaCoO_3$	$La(OH)_3$	La_2O_3	La_2O_3	–	$La_4Co_3O_{10}$, La_2O_3
20%Sr	$(La,Sr)_2CoO_4$	$(La,Sr)_2CoO_4$	$(La,Sr)_2CoO_4$	–	$(La,Sr)_2CoO_4$
20%Ca	$(Ca_3Co_2O_6)$	CaO	$(La,Ca)_2CoO_4$	$(La,Ca)_2CoO_4$, '*liq. Ca–Co–O*'	–
Co-excess					
$LaCoO_3$	Co_3O_4	CoO, *La–Si–O*	CoO, *La–Si–O*	–	–
G/N-samples					
Stoichiometric					
$LaCoO_3$	(none)	(CoO, *La–Si–O*)	(CoO, *La–Si–O*)	–	–
20%Sr	(none)	(CoO)	(CoO)	–	–
20%Ca	(Co_3O_4)	(CoO)	(CoO, '*liq. Ca–Co–O*')	–	–

[a] Minor secondary phases are given in brackets.
[b] Phases written in italics are identified by EDS, and others are identified by XRD.

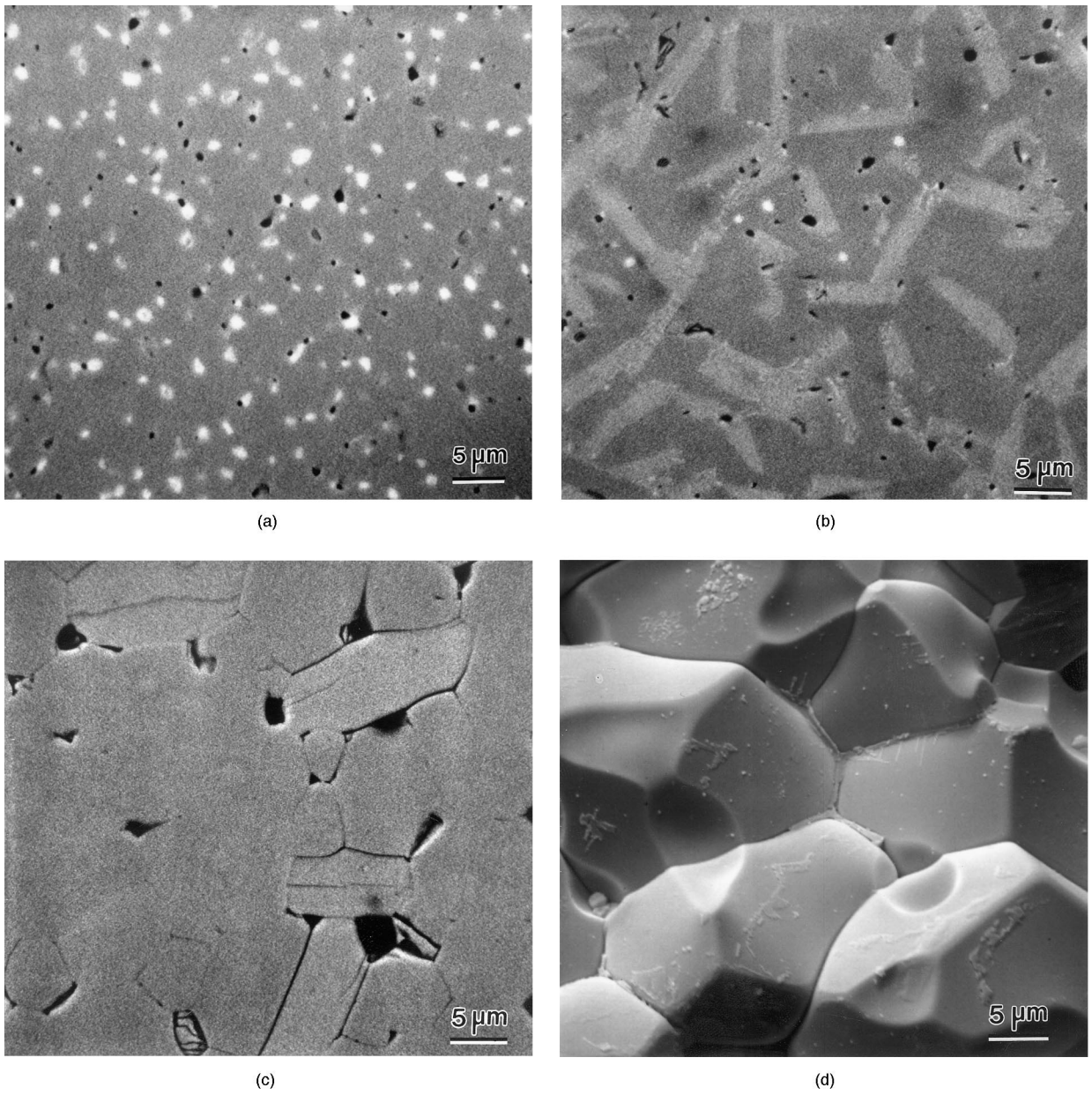

Fig. 1. SEM images of polished surfaces or fracture surface of Co-deficient samples sintered for 2 h. (a) $LaCoO_3$ at 1350°C, (b) $LaCoO_3$ at 1450°C, (c) 20%Ca at 1350°C and (d) 20%Ca at 1400°C.

of Co-deficient 20%Sr (Table 2) is not significantly altered during sintering of the calcined powders. CoO was observed in sintered 20%Sr G/N-samples indicating that this material is Co-excess relative to the perovskite stoichiometry.

3.1.3. 20%Ca

The Co-deficient 20%Ca powder contained the phase $Ca_3Co_2O_6$ in addition to the perovskite after calcination (Table 2). The Ca-content in the perovskite phase is lower than 20 mol% according to the chemical analysis and the presence of $Ca_3Co_2O_6$. The phase composition of Co-deficient 20%Ca was observed to change with increasing sintering temperature. After sintering at 1200°C, CaO with some solid solution of CoO was observed in addition to the major perovskite phase. This is probably due to the phase equilibrium:

$$yCa_3Co_2O_6(s) + LaCoO_3(s) = yCaO(s) + LaCa_{2y}Co_{1+2y}O_{3+5y}(s) \quad (2)$$

Only Co(III) is assumed in perovskite, and the initial content of Ca in $LaCoO_3$ and solid solution of CoO in CaO[18] are neglected here. The driving force of reaction (Eq. 2) is probably the decomposition of $Ca_3Co_2O_6$, reported at 1026°C in air.[18] A new phase with composition $(La_{0.6}Ca_{0.4})_2CoO_4$ (Table 2) with unknown structure

was observed after sintering at 1350°C, shown in Fig. 1(c). The observed XRD pattern cannot be interpreted to any known phase. However, the chemical composition found by EDS indicates that the phase is of K_2NiF_4 type. The chemical reaction taking place during heating to 1350°C is proposed to be

$$CaO(s) + LaCoO_3(s) = LaCaCoO_4(s) \quad (3)$$

Here, the solid solution of CoO in CaO and the Ca-content in $LaCoO_3$ are neglected. The change in the phase composition is probably due to a reduction of the mean valance state of Co with increasing temperature, which is neglected in reaction (Eq. 3).

A liquid phase has probably been formed in Co-deficient 20%Ca during sintering at 1400°C as shown in Fig. 1(d). The only relevant stable liquid reported in the literature is the eutectic at 1350°C and 65 mol% CoO in the pseudo binary phase diagram CaO-CoO.[18] A melt with approximate composition $Co_{0.65}Ca_{0.35}O$ is therefore proposed formed by a reaction between the perovskite and the K_2NiF_4-type phase. This is a reasonable explanation of the observed liquid phase in the sintered Co-deficient 20%Ca sample at 1400°C [see Fig. 1(d)].

In the Co-excess 20%Ca G/N-sample CoO was observed at 1200°C (see Table 2) and a liquid phase was observed after sintering at 1350°C. The precursor for the liquid phase is probably CoO(ss), which melts incongruently at a temperature near 1350°C depending on the Ca content.[18] The formation of a melt with approximate composition $Co_{0.65}Ca_{0.35}O$[18] would result in evolution of oxygen gas due to the reduction of the valance state of cobalt. This may explain the formation of the large pores observed after sintering at 1350°C.

Impurities of sulfur and silicon were observed in some of the sintered samples (Table 2). Sulfur originates from the EDTA used in the preparation of the powders. Silicon was mostly observed in pure $LaCoO_3$ and in larger amounts in the Co-excess composition.

The composition of the silicon containing phase measured by EDS was $La_{3.7}Si_{2.4}Co_{1.0}O_x$, but the observed XRD pattern could not be interpreted to any known phase. The silicon is most probably pollution from the mullite-tube in the furnace used during calcination of the powders. A reducing atmosphere may occur during calcination due to residual carbon from the synthesis, and this will result in formation of SiO(g) which may react with the perovskite powders.

3.2. Densification behaviour

Linear shrinkage and differential linear shrinkage during sintering at a constant heating rate of the three near stoichiometric G/N-samples are shown in Fig. 2. The densities after sintering were 79.4, 99.7 and 89.5% for $LaCoO_3$, 20%Sr and 20%Ca, respectively. $LaCoO_3$ sinters in a broader temperature interval than the Ca/Sr-substituted $LaCoO_3$. $LaCoO_3$ has only a single broad shrinkage event, while two sintering mechanisms are evident for the two other compositions (Fig. 2). The event observed at about 900°C for 20%Sr might be due to a solid state phase transition, while the second event observed at 1300–1350°C for 20%Ca is probably due to formation of the liquid CoO–CaO phase leading to liquid phase sintering.

The densification of $LaCoO_3$ based ceramics is shifted to lower temperatures when $LaCoO_3$ is substituted by Sr or Ca. It is unlikely that diffusion of oxygen is rate

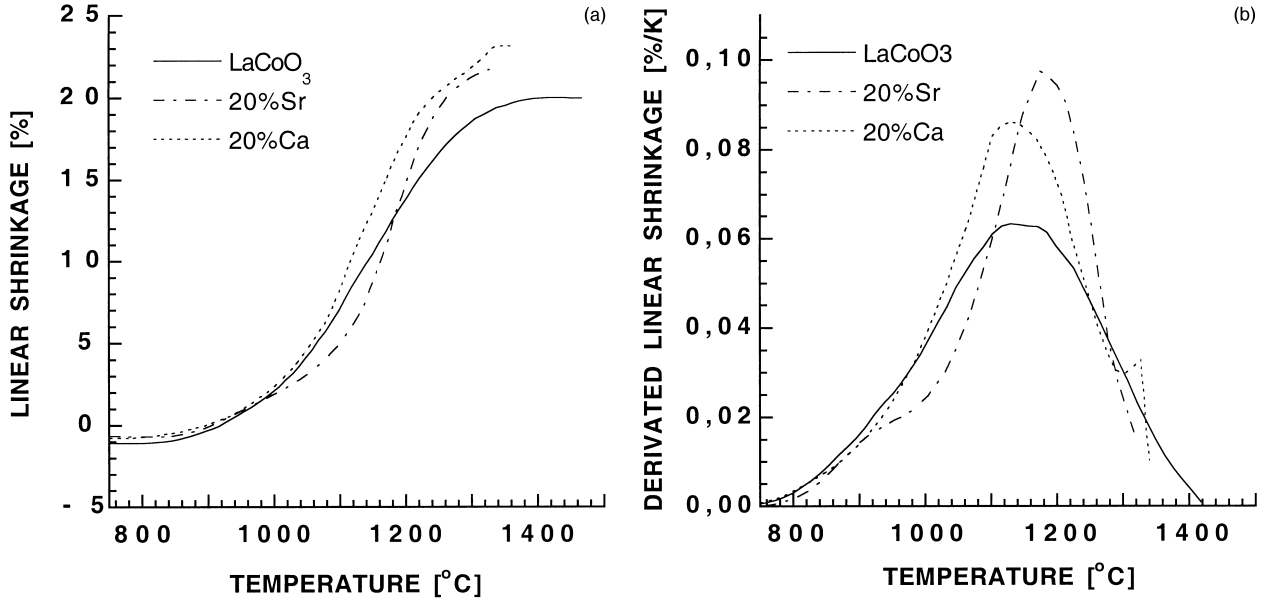

Fig. 2. (a) Linear shrinkage and (b) differential linear shrinkage during sintering of near stoichiometric G/N-powders; $LaCoO_3$, 20%Ca and 20%Sr. The heating rate is 120 K/h.

limiting during sintering since the materials are oxygen conductors even though the oxygen vacancy concentration increases with Ca/Sr-substitution. It is more probable that diffusion of the large A-cations are rate determining. By substitution of Sr and Ca the symmetry changes from hexagonal towards a more cubic structure shown by the decreasing rhombohedral angle (Rhombohedral angles obtained from the X-ray diffraction patterns are 60.79°, 60.55° and 60.68° for $LaCoO_3$, 20%Sr and 20%Ca, respectively). One could speculate that diffusion of cations increases with increasing symmetry since the average coordination number of the A-cations is highest in the cubic perovskite structure.

The densification of the G/N-powders was further investigated at isothermal conditions at 1050, 1200 and 1350°C based on the results in Fig. 2. Densification of EDTA-powders was investigated in the temperature interval 1200–1450°C. The density as a function of temperature for near stoichiometric, Co-excess and Co-deficient EDTA-samples is given in Fig. 3. The corresponding density of G/N-samples is given in Fig. 4. The crystallographic densities for stoichiometric samples, indicated by broken lines, were calculated from lattice parameters refined from XRD patterns of stoichiometric samples sintered at 1200°C.

Near 100% of theoretical density was obtained for near stoichiometric $LaCoO_3$ after sintering at 1350°C (Fig. 3), while lower densities are obtained for the non-stoichiometric samples. The theoretical density of the Co-deficient material is lower due to the lower low crystallographic density of the secondary phases La_2O_3 and $La_4Co_3O_{10}$. The evolution of $O_2(g)$ in Eq. (1) does not lead to increased porosity, probably due to slow reaction or due to enhanced grain boundary diffusion of oxygen. At Co-excess a higher porosity is observed. The presence of CoO inhibits sintering of the material. The melting point for CoO is considerably higher than for $LaCoO_3$, and the sintering temperature will be higher for the two-phase mixture than for single phase $LaCoO_3$. The corresponding explanation holds for Co-deficient $LaCoO_3$ at 1200°C where La_2O_3 is present. The $LaCoO_3$ G/N sample also

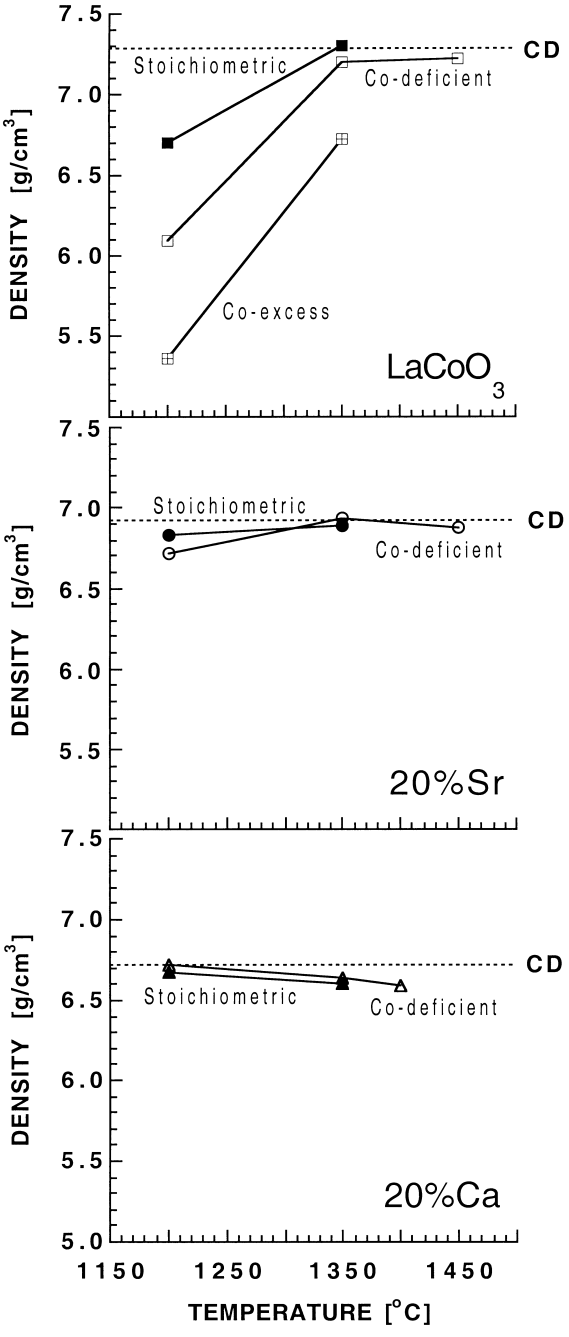

Fig. 3. Density after 2 h sintering at different temperatures for near stoichiometric (filled symbols), Co-deficient (open symbols) and Co-excess (crossed symbols) $LaCoO_3$, 20%Ca and 20%Sr. The powders were prepared by the EDTA-method. Crystallographic density is indicated by broken lines ($LaCoO_3 > 20\%Sr > 20\%Ca$). Crystallographic density was calculated from the hexagonal unit cell parameters a and c (Å) ($LaCoO_3$: 5.444 and 13.097, 20%Sr: 5.448 and 13.179 and 20%Ca: 5.432 and 13.101).

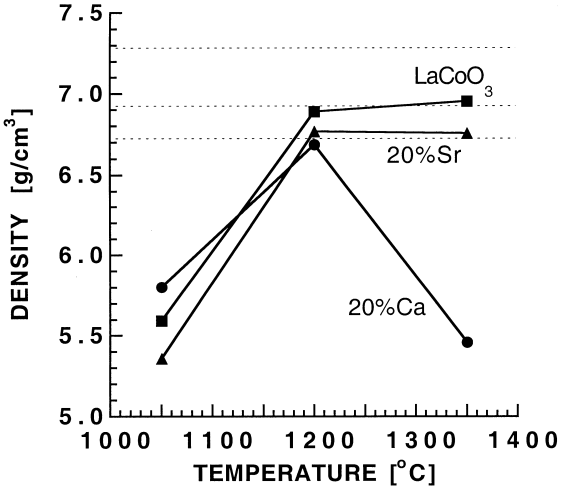

Fig. 4. Density after 2 h sintering at different temperatures for $LaCoO_3$, 20%Ca and 20%Sr. The powders were prepared by the G/N-method. Crystallographic densities are indicated by broken lines (LaCoO3) > 20%Sr > 20%Ca).

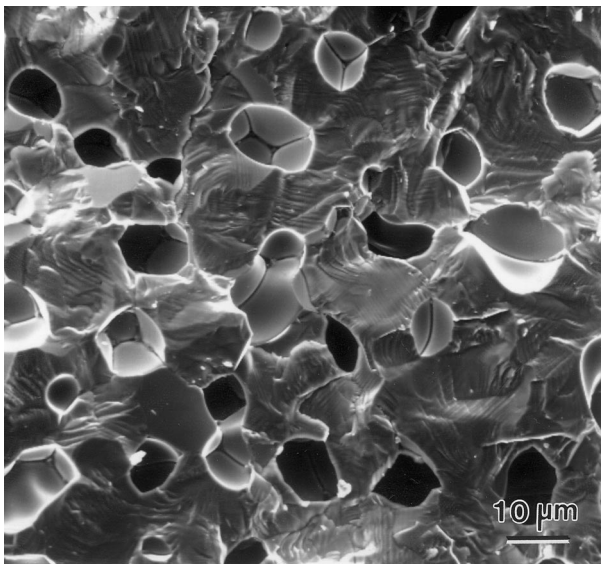

Fig. 5. Fracture surface of 20%Ca ceramic sintered at 1350°C for 2 h. The powder used was prepared by the G/N-method.

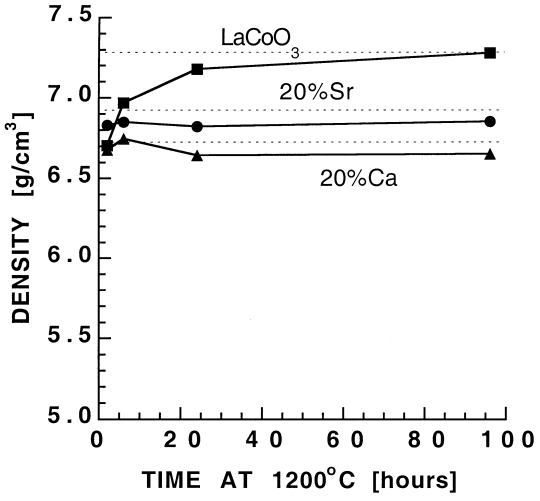

Fig. 6. Density after isothermal sintering for 2–96 h at 1200°C for near stoichiometric $LaCoO_3$, 20%Ca and 20%Sr. Powders were prepared by the EDTA-method. Crystallographic densities are indicated by broken lines ($LaCoO_3$ > 20%Sr > 20%Ca).

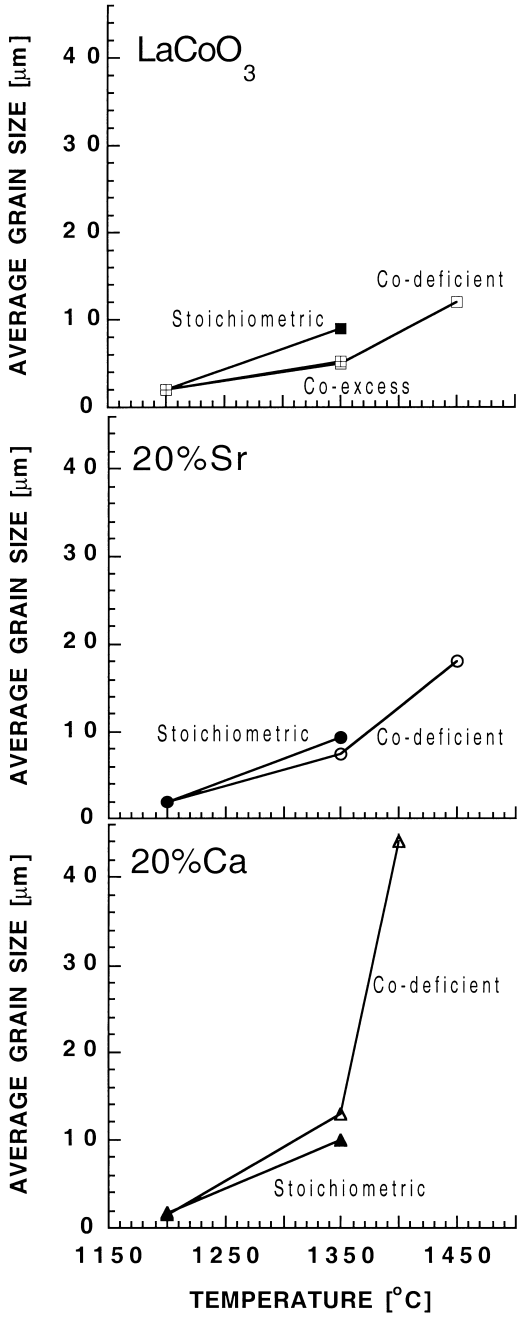

Fig. 7. Average grain size after sintering for 2 h at 1200–1450°C for near stoichiometric (filled symbols), Co-deficient (open symbols) and Co-excess (crossed symbols) $LaCoO_3$, 20%Ca and 20%Sr. Powders were prepared by the EDTA-method.

obtains a lower density than the near stoichiometric EDTA-sample. This is either due to a small Co-excess or larger initial particle size in the G/N-powder.

Both near stoichiometric and Co-deficient 20%Sr obtain high density in the whole temperature interval 1200–1450°C as can be seen from Figs. 3 and 4. The G/N-sample has slightly lower density, which is due to the small Co-excess or larger initial particle size.

Near stoichiometric and Co-deficient 20%Ca samples are nearly 100% dense after sintering at 1200°C, but the density slightly decreases with increasing sintering temperature (Fig. 3). The G/N-sample shows a more distinct trend (Fig. 4), and obtains a high porosity after sintering at 1350°C as shown in Fig. 5. The difference in porosity might be due to Co-excess indicated by the presence of Co_3O_4 in the calcined G/N powder. A reduction of cobalt takes place during the formation of the CaO–CoO eutectic melt and O_2(g) is formed. The evolution of the gas after pore closure might explain the high porosity observed at 1350°C. Evolution of gas due to volatile contaminates cannot be excluded as an alternative explanation of the high porosity.

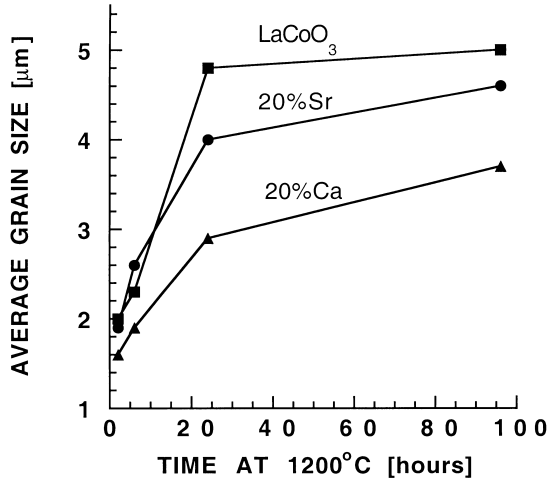

Fig. 8. Average grain size after isothermal sintering for 2–96 h at 1200°C for near stoichiometric $LaCoO_3$, 20%Sr and 20%Ca. The powders were prepared by the EDTA-method.

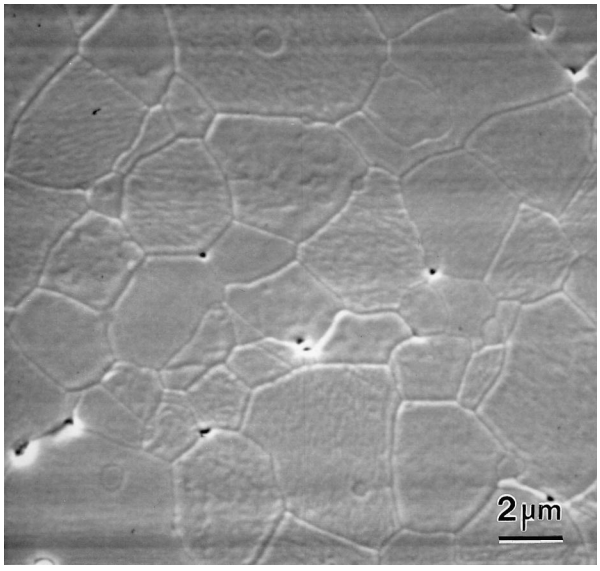

Fig. 9. SEM image of a thermally etched polished section of near stoichiometric $LaCoO_3$ sintered at 1200°C for 96 h. The powder was prepared by the EDTA-method.

Prolonged isothermal sintering at 1200°C for near stoichiometric materials increase the density for $LaCoO_3$ as shown in Fig. 6. 20%Sr and 20%Ca are already dense after 2 h.

3.3. Microstructure

The average grain size for EDTA-samples after sintering for 2 h in the temperature range 1200–1450°C is presented in Fig. 7. A larger extent of grain growth above 1200°C is observed in the substituted materials compared to $LaCoO_3$.

Smaller average grain size is observed in Co-excess and Co-deficient $LaCoO_3$ compared to near stoichiometric samples. The smaller grain size at non-stoichiometry is due to the presence of La_2O_3 or CoO acting as grain growth inhibitors by pinning the grain boundaries. At Co-excess micro cracking is observed, probably due to differences in thermal expansion of the two phases during cooling.

In 20%Sr samples the phase $(La,Sr)_2CoO_4$ is pinning the grain boundaries at Co deficiency, and therefore smaller grains are observed at Co-deficiency compared to the near stoichiometric samples (Fig. 7).

20%Ca shows the opposite behavior, and larger extent of grain growth has occurred at Co-deficiency compared to at near stoichiometry (Fig. 7). A change in sintering temperature and stoichiometry also has a stronger effect on the microstructure for 20%Ca than for the other compositions. This difference can be explained by the changes in phase composition during heating. The abrupt increase in grain size between 1350 and 1400°C at Co-deficiency is due to the presence of the liquid $Ca_{1-x}Co_xO$ phase described earlier. The liquid phase located at the grain boundaries can be seen in Fig. 1(d). Presence of a liquid phase enhances the mass transport leading to exaggerated grain growth in this case. The larger grains in the Co-deficient sample compared to the near stoichiometric sample sintered at 1350°C might be due to the reaction taking place between 1200 and 1350°C at Co-deficiency [Eq. (3)] leading to formation of relatively large amounts of $(La,Ca)_2CoO_4$ (Fig. 1c). This chemical reaction during sintering explains the opposite trends observed between Co-deficiency and near stoichiometry at 1350°C in Sr and Ca substituted compositions.

The microstructure of near stoichiometric $LaCoO_3$ and 20%Sr is qualitatively equal for the G/N-samples and EDTA-samples, however for 20%Ca at 1350°C the G/N-sample has twice as large grains (20 μm) compared to the near stoichiometric EDTA-sample. Additionally large pores are formed as was shown in Fig. 5. As discussed earlier this might be due to evolution of gas during the formation of a molten phase.

Fig. 8 shows how the grain size develops with time at 1200°C for near stoichiometric EDTA-samples. After approximately 24 h the grain growth has ceased, and the resulting grain size after 96 h is in the range 3–5 μm. Pores are mainly located at the grain boundaries, (Fig. 9). A qualitatively similar microstructure was observed for the three G/N samples sintered at 1200°C.

4. Conclusions

Substitution of La with Sr or Ca in $LaCoO_3$ decreases the sintering temperature. Near 100% dense materials are obtained for all compositions apart from the Co-excess $LaCoO_3$, though at different temperatures. The phase relations in the La–Co–O and Ca-Co-O systems

make it important to control the cation stoichiometry in order to avoid formation of secondary phases. In Ca substituted samples a small deviation from stoichiometry leads to formation of a liquid phase and exaggerated grain growth at high temperature. Presence of secondary phases may lead to cracking of the material and decline the functional properties. Preparation of dense and phase pure $LaCoO_3$ based ceramics is a demanding task, and dense single phased materials with small grains are obtained in a narrow temperature interval and a highly controlled cation stoichiometry is required.

Acknowledgement

Financial support from the Research Council of Norway is appreciated.

References

1. Ohno, Y., Nagata, S. and Sato, H., Properties of oxides for high temperature solid electrolyte fuel cells. *Solid State Ionics*, 1983, **9/10**, 1001–1008.
2. Muller, S., Striebel, K. and Haas, O., $La_{0.6}Ca_{0.4}CoO_3$: a stable and powerful catalyst for bifunctional air electrodes. *Electrochim. Acta*, 1994, **39**, 1661–1668.
3. Lindstedt, A., Strømberg, D. and Milh, M. A., High-temperature catalythic reduction of nitrogen monoxide by carbon monoxide and hydrogen over $La_{(1-x)}Sr_{(x)}MO_3$ perovskites (M = Fe, Co) during reducing and oxidising conditions. *Appl. Cat. A: General*, 1994, **116**, 109–126.
4. Balachandran, U., Dusek, J. T., Mieville, R. L., Poeppel, R. P., Kleefish, M. S. and Pei, S., Dense ceramic membranes for partial oxidation of methane to syngas. *J. Appl. Catalysis*, 1995, **133**, 19–29.
5. Gödickemeier, M., Sasaki, K. and Riess, L., Perovskite cathodes for solid oxide fuel cells based on ceria electrolytes. *Solid State Ionics*, 1996, **86/88**, 691–701.
6. Chen, C. H., Bouwmeester, H. J. M., van Doorn, R. H. E., Kruidhof, H. and Burggraaf, A. J., Oxygen permeation of $La_{0.3}Sr_{0.7}CoO_{(3-\delta)}$. *Solid State Ionics*, 1997, **98**, 7–13.
7. Koc, R. and Anderson, H. U., Liquid phase sintering of $LaCrO_3$. *J. Euro. Ceram. Soc.*, 1992, **9**, 285–292.
8. Denos, Y., Morin, F. and Trudel, G., Characterisation of pure and strontium substituted lathanum cobaltites synthesised by the glycine–nitrate process. *Proc. Electrochem. Soc.*, 1993, **93/94**, 231–240.
9. Janecek, J. J. and Wirtz, G. P., Ternary compounds in the system La–Co–O. *J. Am. Chem. Soc.*, 1978, **61**, 242–244.
10. Kitayama, K., Thermogravimetric study of the Ln_2O_3–Co–Co_2O_3 system. IV: Ln = La at 1100 and 1150°C. *J. Solid State Chem.*, 1997, **131**, 18–23.
11. Kitayama, K., Thermogravimetric study of the Ln_2O_3–Co–Co_2O_3 system. I: Ln = La. *J. Solid State Chem.*, 1988, **73**, 381–387.
12. Seppädnen, M., Kyto, M. and Taskinen, R., Stability of the ternary phases in the LaCo–O system. *Scan. J. Met.*, 1979, **8**, 199–204.
13. Petrov, A. N., Cherpanov, V. A., Zuyev, A. Y. and Zhukovsky, V. M., Thermodynamic stability of ternary oxides in Ln–M–O (Ln = La, Pr, Nd; M = Co, Ni, Cu) systems. *J. Solid State Chem.*, 1988, **77**, 1–14.
14. Morin, F., Trudel, G. and Denos, Y., The phase stability of $La_{0.5}Sr_{0.5}CoO_{3-\partial}$. *Solid State Ionics*, 1997, **96**, 129–139.
15. Munakata, F., Takahashi, H., Akimune, Y., Shichi, Y., Tanimura, M., Inoue, Y., Rittaporn, I. and Koyama, Y., Electronic state and valence control of $LaCoO_3$: difference between La-deficient and Sr-substituting effects. *Phys. Rev. B*, 1997, **56**, 979–982.
16. Chick, L. A., Pederson, L. R., Maupin, G. D., Bates, J. L., Thomas, L. E. and Exarhos, G. J., Glycine-nitrate combustion synthesis of oxide ceramic powders. *Mater. Lett.*, 1990, **10**, 6–12.
17. Aukrust, M. and Muan, A., Thermodynamic properties of solid solutions with spinel-type structure. I, The system Co_3O_4–Mn_3O_4. *Trans. AIME*, 1964, **230**, 378–382.
18. Woermann, E. and Muan, A., Phase equlibria in the system CaO–Cobalt oxide in air. *J. Inorg. Nucl. Chem.*, 1970, **32**, 1455–1459.